https://doi.org/10.20965/jdr.2019.p0766

Paper:

Comparative Petrological Studies of 1962 and 1988–1989 Eruptions of Tokachidake Volcano, Japan: A Case Study for Understanding the Relationship Between Eruption Style and Magma Processes

Mitsuhiro Nakagawa[*,†], **Akiko Matsumoto**[*], **Kyohei Kobayashi**[*,**], **and Keiji Wada**[***]

[*]Department of Natural History Sciences, Graduate School of Science, Hokkaido University
N10W8 Kita-ku, Sapporo, Hokkaido 060-0810, Japan
[†]Corresponding author, E-mail: mnakagawa@sci.hokudai.ac.jp
[**]Koken Engineering Co., Ltd., Sapporo, Japan
[***]Earth Science Laboratory, Hokkaido University of Education, Asahikawa, Japan

[Received March 14, 2019; accepted June 25, 2019]

Repeated magmatic eruptions of Tokachidake volcano have caused severe volcanic disasters on three occasions during the 20th century. To prepare for the next eruptive activity, understanding the structure of the magma plumbing system by using petrological analysis of juvenile materials is crucial. Here, we perform petrological analysis of juvenile materials to investigate the difference between two contrasting eruptions in 1962 and 1988–1989, respectively. All these juvenile materials are composed of mafic andesite, which were formed by mixing of olivine-bearing basaltic and pyroxene andesitic magmas. The compositional zonations of olivine phenocrysts in all of these rocks suggest that the injection of the basaltic magma into the andesitic magma occurred several months prior to the 1962 eruption and about six months before the 1988–1989 eruption. In the case of the 1962 activity, the mixed magma rapidly ascended without stagnation from the magma chamber and erupted as a sub-Plinian type. However, the juvenile materials of the 1988–1989 eruptions show distinct petrological features such as higher crystallinity of the matrix, orthopyroxene reaction rims around the olivine, and overgrowth mantle zones around Ti-magnetite phenocrysts. These features suggest that the mixed magma ascended slowly and possibly stagnated at shallower levels prior to eruption. The stagnated magma became a cap rock of the vent system and caused a series of Vulcanian eruptions. These distinct modes of magma ascent can be explained by differences in the magma supply rate. In the case of the 1962 eruption, the volume of magma that erupted in a period of less than 24 h was 7.1 × 10^7 m^3. On the contrary, 23 explosions occurred over three months of the 1988–1989 activity and generated 1 × 10^5 m^3 of ejecta including juvenile and non-juvenile materials. These large eruption rate differences can be attributed to the distinct ascent rates of the magma between the two eruptive activities.

Keywords: Tokachidake volcano, eruption style, magma mixing, compositional zonation of olivine, mode of magma ascent

1. Introduction

Tokachidake volcano, one of the most active volcanoes in Japan, produced three magmatic eruptions that caused severe volcanic disasters during the 20th century in 1926, 1962, and 1988–1989, respectively. In the 1926 eruption, sector collapse of the edifice caused a large lahar that ran to the foot of the volcano and killed 144 people. This disaster was the most severe volcanic event in Japan during the 20th century. Although obvious eruptions have not occurred after the 1988–1989 activity, vigorous fumarole activity at recent craters indicates the beginning of the next eruptive activity.

Understanding the processes of the magma plumbing systems beneath a volcano is crucial for mitigating a volcanic disaster caused by the next eruption. The historical precursory phenomenon and eruption sequence of each eruption of Tokachidake volcano have been well summarized [1–3]. Moreover, geophysical monitoring of the volcano has been developed after the 1962 eruption [4]. In addition, geophysical and geochemical studies have recently clarified the structure of the hydrothermal system beneath the volcano [5, 6]. Although the general petrological features of Holocene rocks from the Tokachidake volcano eruption have been revealed [7, 8], detailed petrological studies focusing on these historic eruptive rocks have not been performed. Petrological and geochemical studies for the eruptive materials are essential for understanding the present state of magma plumbing systems beneath volcanoes, as in the case of recent eruptions of Usu [9, 10], Hokkaido–Komagatake [11], Miyakejima [12], and Shinmoe-dake volcanoes [13, 14].

Although the rocks from the historic eruptions are similar mafic andesite, the modes of these eruptions differ

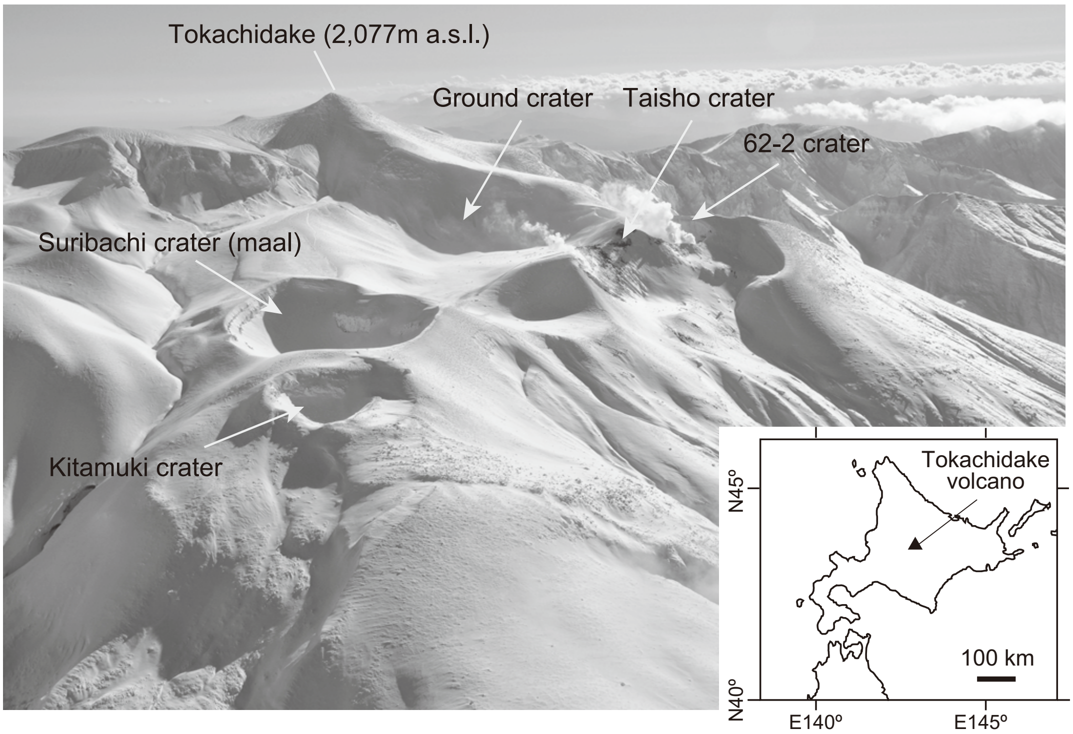

Fig. 1. Photograph of the Tokachidake volcano captured from the northwestern sky. The inset map shows the location of Tokachidake volcano.

Table 1. Summary of the magmatic eruptive activity at Tokachidake volcano during the 20th century.

Eruption age (AD)	Vent	Eruption style	Remarks
1926–1928	Taisho	Phreatomagmatic eruption Edifice collapse with mud flow	Total of 146 people were killed.
1962	62-0–62-4	Magmatic eruption (sub-Plinian)	ca 12,000 m column height 5 persons were killed.
1988–1989	62-2	Magmatic eruption (Vulcanian and Strombolian) accompanied with pyroclastic flow and surge	Ballistic bombs up to 20 m were erupted.

significantly. To investigate the relationship between the magma processes and the eruption mode, we focus on the contrasting 1962 and 1988–1989 eruptions. The former eruption was a relatively large sub-Plinian eruption, whereas the latter was a series of small Vulcanian eruptions. In this study, we present the petrography, whole-rock and mineral chemistry of the eruptive rocks from the two eruptions. We clarify that the petrological difference between these eruptions can be explained by their distinct modes in magma ascent processes. These results are crucial for mitigating volcanic disasters caused by the future eruptive activity of the Tokachidake volcano.

2. General Geology

The Tokachidake volcano is situated at the central part of the Tokachidake Volcano Group, central Hokkaido, located at the southwestern end of the Kuril arc (**Fig. 1**). The activity of the volcano group began about 1 Ma and has continued through the present. The group consists of more than 10 volcanic edifices each 5–10 km in diameter. Younger eruption centers since the latest Pleistocene are distributed around the Tokachidake edifice. The most explosive eruptions in Holocene occurred 4.7 ka and 3.3 ka at the northwestern flank of the edifice, which formed the Ground craters. Afterward, the eruption centers migrated, and magmatic eruptions have occurred intermittently at several craters. During the 20th century, magmatic eruptions have occurred three times at the Taisho crater and at the 62 craters (**Fig. 1**).

Although the juvenile materials of historical eruptions are similar mafic andesite, each eruption type was different (**Table 1**) [1, 2]. In the 1926 eruption, the sector collapse of a cinder cone with fallout deposits produced a debris avalanche and a mud flow [15]. The mud flow, travelling 25 km from the Taisho crater, destroyed forests, farms, and a town [16]. After the sector collapse, small explosive eruptions occurred intermittently to erupt small amounts of juvenile materials at an estimated volume of 1.3×10^4 m^3 (**Table 1**) [3].

Sub-Plinian eruptions occurred in 1962, forming the aforementioned 62 craters (62-0–4; only 62-2 and 62-3 craters still exist: **Fig. 1**). The climactic eruption continued for less than one day, and the eruption column reached 12 km above the crater. Ash fall deposits derived from the column were widely distributed in the eastern area of Hokkaido. This eruption was the most voluminous of the 20th century, with a total ejecta volume of 7.1×10^7 m^3 [17] and a composition of mainly juvenile materials.

A small phreatomagmatic eruption occurred in December 1988, with the eruptive activity continuing to the following year. By March 1989, 23 Vulcanian-type explosions were recorded [2]. These explosions produced small pyroclastic flow and surge deposits as well as ejected ballistic bombs around the 62-2 crater (**Fig. 1**). The total estimated volume of ejecta was 6×10^5 m^3 (**Table 1**) [2]. However, the volume of juvenile materials in the 1988–1989 eruptions was estimated to be about 1.2×10^5 m^3 because the proportion of juvenile materials in the eruptive rocks was estimated to be 20% [2].

3. Samples and Experimental Procedures

Juvenile materials of the 1962 eruptions were collected near the Taisho and 62-2 craters. Eruptive rocks from the 1988–1989 event were collected in 1989 following the eruptive activity [7]. The juvenile materials from these eruptions are similar mafic andesitic scoriae. Compared with the 1962 juvenile materials, the 1988–1989 ones are usually less porous; dense mafic andesite lithics were often recognized. In addition, glassy rocks with a peculiar feature formed by the melting of altered volcanic rocks were also found [7].

Thin sections of more than 20 samples were made for petrological analysis. The modal analysis was based on more than 3000 counts per thin section. The proportions of phenocrystic minerals and matrix were calculated on a vesicle-free basis. Analysis of mineral compositions and back-scattered electron image (BEI) observation for representative thin sections were conducted using wavelength dispersive-type electron microprobes, JEOL JXA-8800R and JXA-8530F, at Hokkaido University. Analysis was undertaken with an accelerating voltage of 15 kV and beam currents of 10 nA for plagioclase and 20 nA for pyroxene, Ti-magnetite, and olivine. All analyses used oxide ZAF correction. Whole-rock chemical compositions were determined on the basis of X-ray fluorescence using a Spectris MagiX PRO system with a Rh tube. The major and trace elements were measured by using glass beads prepared by fusing the sample with an alkali flux composed of a 4 : 1 mixture of lithium tetraborate and lithium metaborate. Major and trace elements were measured for 92 samples diluted to 1 : 2.

4. Petrography and Mineral Chemistry

4.1. General Description

All juvenile materials from the 1962 and 1988–1989 eruptions are phenocryst-rich olivine-bearing orthopyroxene–clinopyroxene basaltic andesites (**Fig. 2**). The modal contents of the phenocrystic minerals of the samples from the 1962 eruption at 40–36 vol.% are slightly lower than those from the 1988–1989 eruption, at 48–44 vol.% (**Table 2**). The phenocrystic and microphenocrystic minerals (> 0.1 mm) include plagioclase (37–26%), orthopyroxene (6.8–2.2%), clinopyroxene (7.6–2.6%), Ti-magnetite (3.0–1.1%), and olivine (1.0–0.3%). Crystal clots composed of plagioclase, pyroxenes, and Ti-magnetite are common in all rocks. Olivine in the samples from the 1962 eruptions always occurs as isolated microphenocrysts (< 0.2 mm) without pyroxene rims, whereas that from the 1988–1989 eruption is usually surrounded by pyroxene rims of various thickness (**Fig. 3**).

The matrix of the rocks from the 1962 eruptions are vesicular and hyalopilitic, whereas those from the 1988–1989 eruption are less vesicular and hyalopilitic. The matrix is composed of pyroxenes, plagioclase, and Ti-magnetite microlites as well as brown glass. Microlites in the 1962 samples are fine and spindle shaped, whereas those in the 1988–1989 ones are relatively large and lath or tabular shaped (**Fig. 2**).

4.2. Mineral Chemistry

(1) Plagioclase

The plagioclase phenocrysts, 0.1–3 mm in length, show various textures such as clear, honeycomb, and resorbed structures. The compositions of the phenocryst cores are nearly the same between the two eruptions, ranging from An92 to An50 (**Fig. 4**). The zonal structures of the phenocrysts are also varied. Phenocrysts with calcic cores show normal compositional zonations, whereas those with less-calcic cores have more calcic rims (**Fig. 5**). These compositional relationships between the core and rim are the same in all samples.

(2) Pyroxenes

The orthopyroxene and clinopyroxene phenocrysts and microphenocrysts are euhedral to subhedral, at 0.1 to 1.0 mm in length. The Mg# ($100 \times \mathrm{Mg}/(\mathrm{Mg} + \mathrm{Fe})$) of most phenocryst cores is 70–76 in the clinopyroxene and 65–75 in the orthopyroxene (**Fig. 4**). Many pyroxene phenocrysts of the samples from the 1962 eruptions show reverse compositional zonation and Mg-rich rims. However, phenocrysts with Mg-rich cores in the 1988–1989 rocks usually have Fe-rich rims, whereas those with Fe-rich cores have Mg-rich rims (**Fig. 5**).

(3) Ti-magnetite

Ti-magnetite phenocrysts and microphenocrysts are common in all samples and are euhedral to subhedral

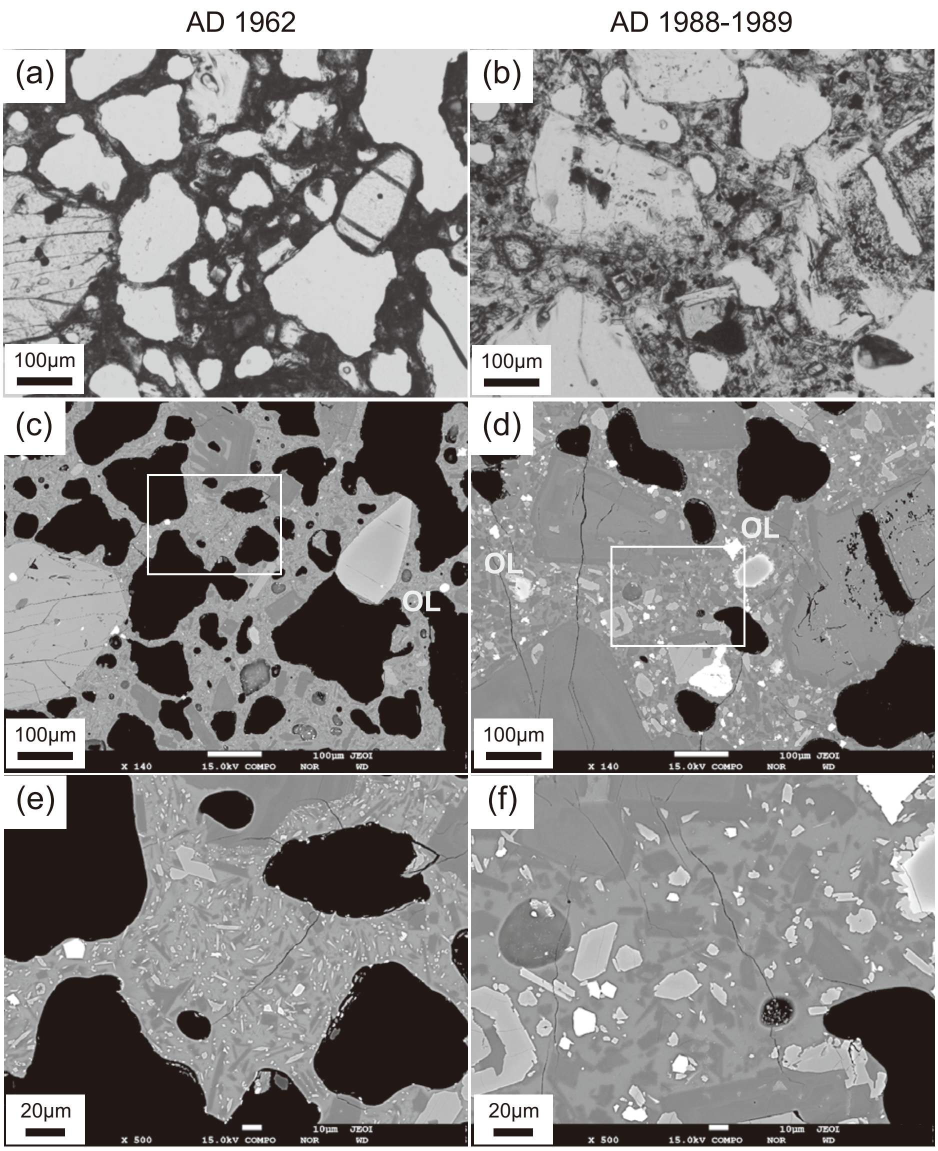

Fig. 2. (a), (b) Microscope photographs and (c)–(f) back-scattered electron images of thin sections of the 1962 and 1988–1989 juvenile materials. The 1962 scoria in (a) and (c) shows a hyalopilitic matrix and an isolated olivine microphenocryst without a pyroxene rim. The matrix contains fine microlites, as shown in (e). On the contrary, the 1988–1989 eruption bomb is characterized by (b), (d) fewer vesicles and (f) higher matrix crystallinity. The olivine microphenocrysts are commonly contained and are surrounded by pyroxene reaction rims, as also shown in **Fig. 3**. Abbreviation: OL, olivine.

at 0.1–0.5 mm in diameter. The Ti-magnetite microlites in the 1962 samples are rare and small, at $< 5\ \mu$m, whereas those in the 1988–1989 samples are common and larger, at 10 μm. The ulvöspinel mole % (X'_{usp}) values and Mg/Mn ratios of the phenocrystic mineral cores of the 1962 samples are 0.29–0.39 and 12–18, respectively (**Figs. 4** and **6**). These phenocrysts do not show clear compositional zonations (**Figs. 5** and **6**). On the other hand, the Ti-magnetite phenocrysts from the 1988–1989 samples show slightly Ti-rich and Mg-poor, $X'_{usp} = 0.32$–0.44 and Mg/Mn = 9–16, respectively. Moreover, these phenocrysts are surrounded by Ti-rich and Mg-poor zones several tens of micrometers in width, at $X'_{usp} = 0.34$–0.48 and Mg/Mn = 6–15), respectively (**Figs. 4** and **6**). Similar zones characterized by distinct chemical compositions such as those in the 1988–1989 sample were not recognized in the phenocrysts of the 1962 samples.

(4) Olivine

The olivine microphenocrysts are euhedral to subhedral at < 0.2 mm and occur in all samples. The modal volume of olivine is less than 1%, and the Fo values ($100 \times \mathrm{Mg}/(\mathrm{Mg} + \mathrm{Fe})$) of the microphenocryst cores range from 70 to 78 in the 1962 samples. These microphenocrysts have Fe-rich rims without reaction rims of the pyroxenes (**Fig. 2(c)**). On the other hand, the olivine microphenocrysts in the 1988–1989 samples have similar magnesian cores, Fo = 71–77, although smaller subhedral olivine microphenocrysts with Fe-rich cores, Fo < 70, were also found (**Figs. 3** and **4**). These olivine microphe-

Table 2. Phenocryst mode and whole-rock chemistry of representative juvenile materials from the 1962 and 1988–1989 eruptive activities at Tokachidake volcano.

Sample No.	890604-5	Tkk 2-2-3	Tkk 2-2-1	Type 3-1	890603-2	040929-3	Type 1-2
Eruption	1962	1962	1962	1988–1989	1988–1989	1988–1989	1988–1989
Type	Bomb	Scoria	Scoria	Bomb Type3	Bomb Type2-3	Bomb Type1	Bomb Type1
Phenocryst mode (vol.%)							
Gms	62.1	59.7	63.9	56.1	56.0	52.0	51.8
Plg	28.2	28.6	26.0	28.3	29.9	34.6	37.2
Cpx	3.6	6.6	6.0	6.0	7.6	6.3	4.0
Opx	3.4	2.9	2.4	6.8	3.3	5.1	4.5
Olv	1.0	0.4	0.6	0.4	0.3	0.3	0.3
Opq	1.7	1.9	1.1	2.5	3.0	1.7	2.1
Whole-rock chemistry (wt.%)							
SiO_2	53.0	53.1	52.2	53.0	52.9	53.3	52.9
TiO_2	1.1	1.1	1.1	1.1	1.1	1.1	1.1
Al_2O_3	17.6	17.9	17.6	17.9	17.7	18.1	17.7
Fe_2O_3	10.5	10.1	10.2	10.0	10.3	10.0	10.3
MnO	0.2	0.2	0.2	0.2	0.2	0.2	0.2
MgO	4.5	4.4	4.5	4.3	4.4	4.3	4.5
CaO	8.9	8.8	8.9	8.8	8.8	8.9	8.8
Na_2O	2.8	2.8	2.8	2.8	2.8	2.8	2.8
K_2O	1.2	1.3	1.3	1.3	1.3	1.3	1.3
P_2O_5	0.2	0.2	0.2	0.2	0.2	0.2	0.2
Total	99.9	99.7	98.9	99.5	99.7	100.1	99.7
(ppm)							
Sc	29.8	31.0	27.5	31.8	31.0	28.7	30.7
V	286	282	274	277	285	278	283
Cr	15.0	14.3	14.1	15.0	16.0	13.3	16.0
Ni	7.8	7.1	6.6	6.7	7.5	6.6	7.7
Rb	32.5	34.2	35.2	34.6	34.3	33.5	34.9
Sr	390	403	394	398	394	392	393
Y	27.8	27.8	26.5	28.0	28.2	28.1	27.5
Zr	99	101	101	101	100	98	99
Nb	4.8	4.6	4.7	4.6	4.9	4.3	4.9
Ba	311	323	314	315	311	313	315

Gms: Groundmass; Plg: Plagioclase; Cpx: Clinopyroxene; Opx: Orthopyroxene; Olv: Olivine; Opq: Opaque minerals.

nocrysts show normal or weak compositional zonation and are surrounded by reaction rims of pyroxenes of various thickness ranging from 2 to 20 μm (**Fig. 3**).

5. Geochemistry

Representative major and trace element variation diagrams of historic juvenile materials from Tokachidake volcano are presented in **Fig. 7**. The major elements are normalized to 100% volatile-free basis with the total iron calculated as FeO. The SiO_2 content of these rocks is 53.2–54.3, which is nearly the same between the two eruptions; the contents of other oxides are also similar between the two events with an apparent linear trend shown in several Harker diagrams.

6. Discussion

6.1. Magma Mixing During the 20th Century

On the basis of disequilibrium petrological features such as the Fe–Mg distribution between Fo-rich olivine (Fo $>$ 75) and pyroxenes and the coexistence of normal and reverse-zoned pyroxenes and plagioclase, Ikeda et al. [7] suggested that the 1988–1989 and 1962 mafic andesites are magma mixing products. Our new data supports their conclusions. Considering the assemblage of the phenocrystic minerals and their compositional relationships, it can be estimated that the mafic andesites are the products of mixing between olivine-bearing basaltic and olivine-free pyroxene andesitic magmas. The basaltic magma might have contained only olivine because the olivine microphenocrysts are always isolated. However,

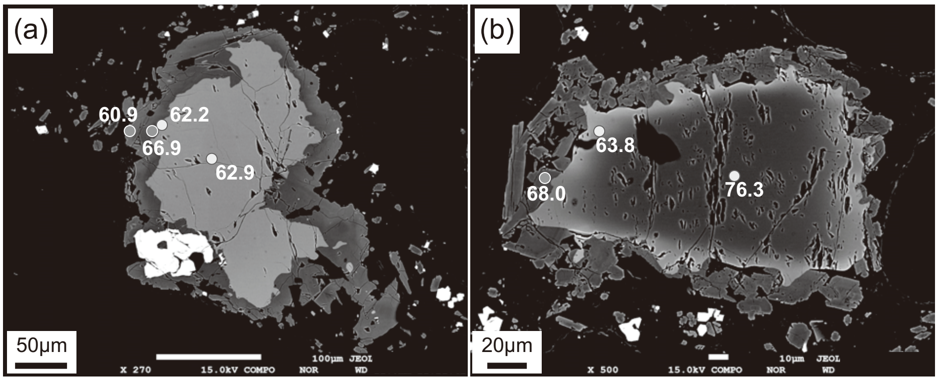

Fig. 3. Back-scattered electron images of olivine microphenocrysts from the 1988–1989 eruption bomb. The numbers in the photographs indicate the Mg# of the olivine (light gray) and orthopyroxene (dark gray). (a) Fe-rich olivine surrounded by a thick orthopyroxene rim. (b) Fo-rich olivine showing normal zonation with an Fe-rich rim. The olivine is surrounded by a thinner orthopyroxene rim.

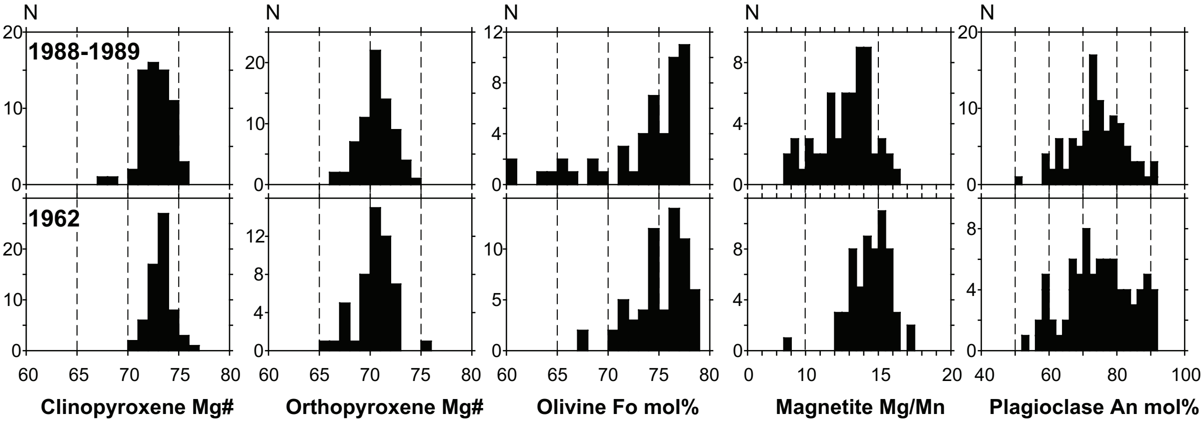

Fig. 4. Histograms of the core compositions of clinopyroxene, orthopyroxene, olivine, Ti-magnetite, and plagioclase phenocrysts and microphenocrysts in the 1962 and 1988–1989 samples. The analysis results of several thin sections from each eruption are summarized in each histogram.

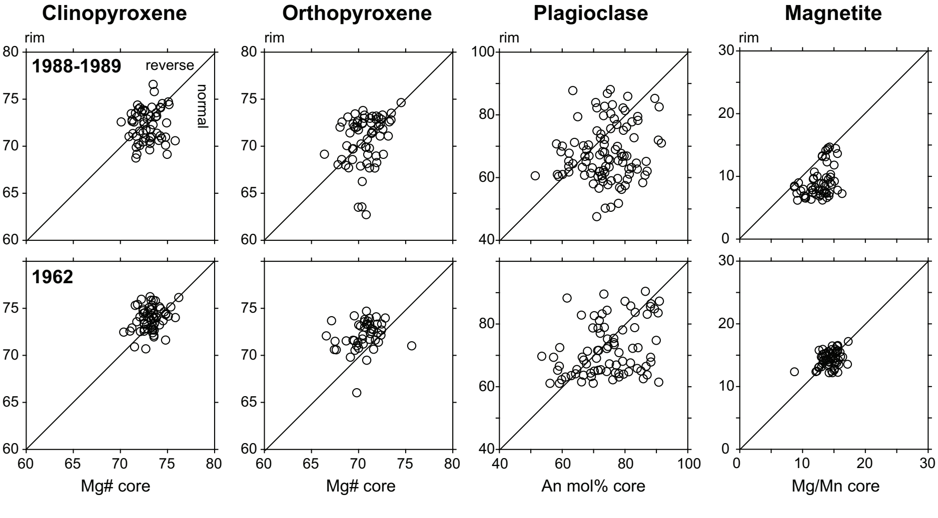

Fig. 5. Diagrams showing the compositional relationship between the core and rim compositions of pyroxenes, plagioclase, and Ti-magnetite phenocrysts in the 1962 and 1988–1989 samples. The analysis results of several thin sections from each eruption are summarized in each diagram.

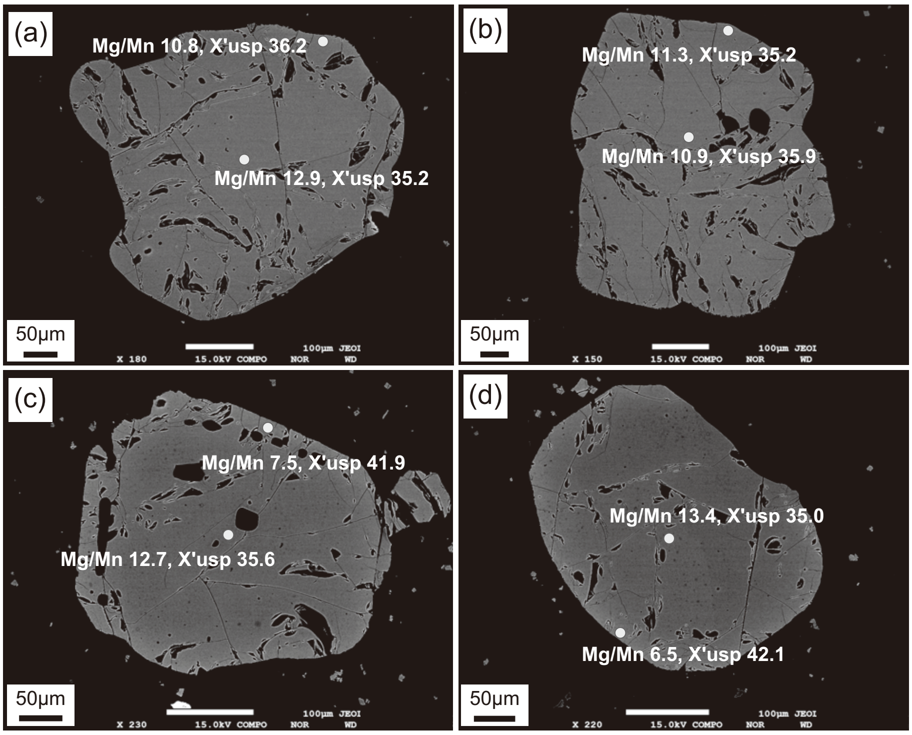

Fig. 6. Back-scattered electron images of Ti-magnetite phenocrysts from the (a), (b) 1962 and (c), (d) 1988–1989 samples. The numbers in the photographs indicate Mg/Mn ratios and ulvöspinel mole % (X'_{usp}). Rims with Ti-rich and low Mg/Mn ratios are recognized in the 1988–1989 sample. The width of the zone is several tens of microns.

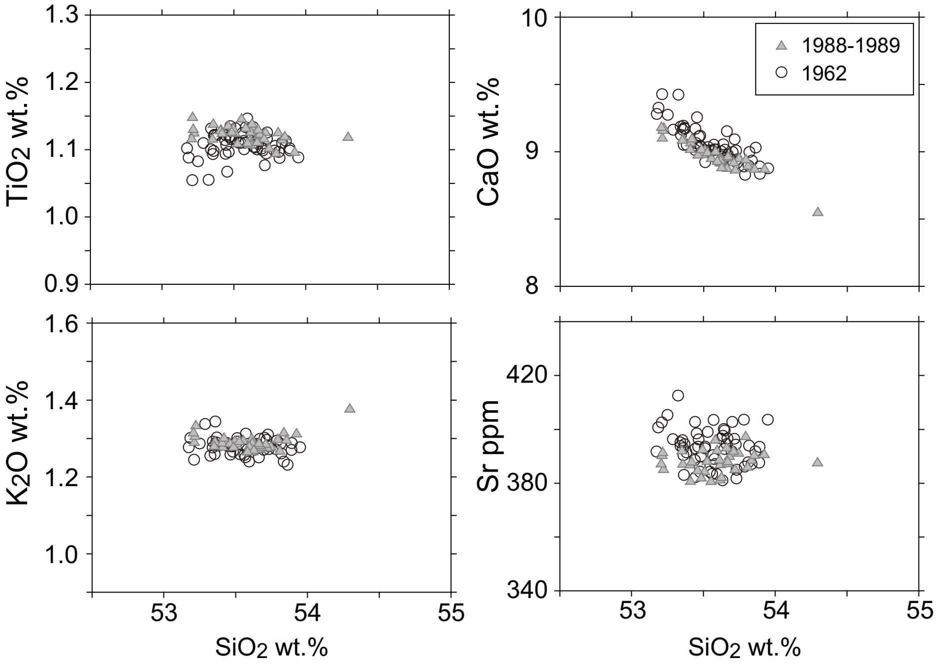

Fig. 7. Selected SiO_2 variation diagrams showing whole-rock major and trace element contents of the 1962 and 1988–1989 juvenile materials of Tokachidake volcano.

the calcic plagioclase is usually derived from basalt because high-An plagioclase, particularly An $>$ 90, crystallizes from basaltic magma at subduction zones [18, 19]. Therefore, we interpreted that the mafic end-member magma was the basaltic magma with olivine and plagioclase phenocrysts, whereas the andesitic magma contained plagioclase, pyroxenes, and Ti-magnetite phenocrysts. This explanation is consistent not only with

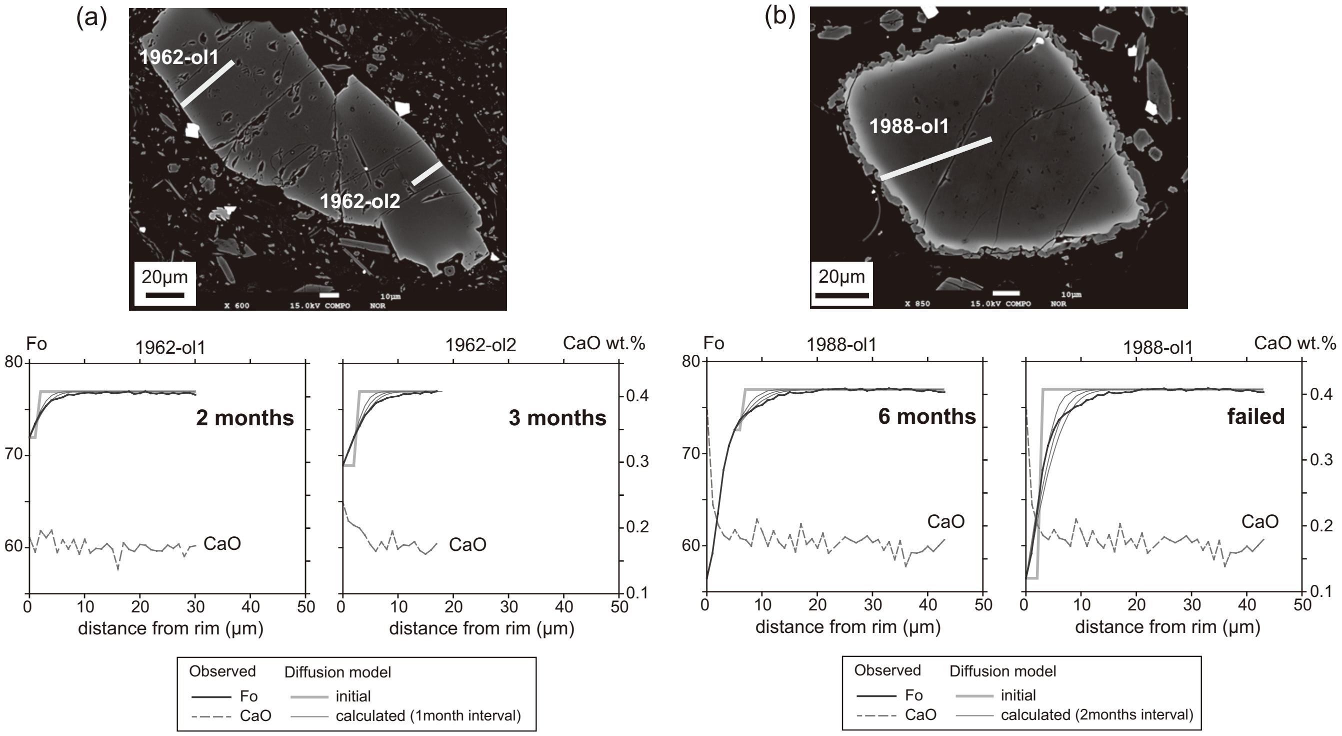

Fig. 8. Zoning profiles and diffusion calculations for olivine microphenocrysts from the (a) 1962 and (b) 1988 samples. The zoning profiles were determined along the direction perpendicular to the [100] or [010] axis inferred from the shape of these phenocrysts (bars in photos). The profile of olivine in the 1988–1989 samples could not be explained by simple diffusion model, owing likely to overgrowth.

the assemblage of crystal clots composed of plagioclase, pyroxenes, and Ti-magnetite but also with the linear trends shown in SiO_2 variation diagrams (**Fig. 7**). In the 1988–1989 samples, Fe-rich olivine microphenocrysts surrounded by thick pyroxene rims are also found. The origin of these Fe-rich olivines will be discussed subsequently.

6.2. Timing of Basaltic Magma Injection During the Two Eruption Episodes

As discussed previously, the basaltic end-member magma that erupted in the 1962 and 1988–1989 eruptions contains high-Fo olivine microphenocrysts (Fo $>$ 75). These olivine phenocrysts always show normal zoning (**Fig. 8**) with decreasing Fo content toward the margin. These zonations were interpreted to have formed by Fe–Mg diffusion between the olivine and the mixed melt after the input of basaltic magma into the andesitic magma. Therefore, we estimated the timing of the magma mixing on the basis of the Fe–Mg elemental diffusion in the olivine microphenocrysts. First, we chose the short axis of each phenocryst on the basis of crystal shape and determined their line profiles along the [100] or [010] axis. Then, we estimated their diffusion times using Fick's second law model [20]. The diffusion coefficient 6.35×10^{-19} m^2/s at 1000°C [21, 22] was used. We assumed the initial condition of Fo content on the basis of the CaO profile because Ca diffusion is slower than Fe–Mg diffusion in olivine [23]. The results of the fitting of the diffusion model are shown in **Fig. 8**.

The olivine microphenocrysts in the 1962 juvenile materials are euhedral without reaction rims (**Fig. 8(a)**), and the diffusion times were about two to three months. In contrast, in the case of the 1988–1989 eruption, all the microphenocrysts have pyroxene reaction rims of various thickness (**Fig. 3**). Therefore, we selected grains with thin reaction rims (**Fig. 8(b)**). However, the line profiles differed from those of the 1962 ones; thus, we were unable to perform the fitting using the simple diffusion model. This suggests that the 1988–1989 olivine was affected by growth. Moreover, the olivine microphenocrysts in the 1988–1989 juvenile materials have Fe-rich outer rims (**Fig. 8(b)**), suggesting the possibility of the olivine overgrowth. According to previous research, the growth rate of olivine is relatively fast, at 10^{-10} m/s at low undercooling, and 10^{-7}–10^{-6} m/s at high undercooling [24]. Therefore, we consider that the overgrowth of olivine occurred after the diffusion of the inner part. We estimated the diffusion time based on the profile from the inner part 5 μm from rim, which shows compositions similar to those of the olivine rims in the 1962 juvenile materials. As a result, its diffusion time is estimated to be about six months. Although we were unable to compare these results owing to the different fitting conditions, we speculate that the duration between the basalt input and the 1988–1989 eruption was relatively longer than for the 1962 event. The

Fe-rich outer rim (Fo < 60) is compositionally in disequilibrium with the rims of co-existing orthopyroxene phenocrysts (**Fig. 5**). This might imply that the overgrowth of olivine and the thin reaction rims, might have occurred just prior to the 1988–1989 eruption, such as that shown by Ti-magnetite as discussed in Section 6.4.

6.3. Andesitic End-Member Magma of the 1988–1989 Eruption

The whole-rock chemical compositions of the 1988–1989 samples are nearly the same as those of the 1962 samples (**Fig. 7**). In addition, the compositional distributions of the cores of the pyroxenes and plagioclase phenocrysts are also the same (**Fig. 4**). Moreover, Fo-rich olivine microphenocrysts (Fo > 75) are commonly recognized in all samples. These suggest that the two end-member magmas of the 1962 and 1988–1989 eruptions were nearly the same. However, as previously mentioned, the rocks of the 1988–1989 eruption show the following distinct petrological features: 1) Fe-rich (Fo < 70) olivine microphenocrysts surrounded by thick pyroxene rims are commonly found (**Fig. 3**); 2) the Mg/Mn ratios of the Ti-magnetite phenocryst cores are lower than those of the 1962 samples (**Figs. 4** and **6**); 3) many pyroxene phenocrysts in the 1962 samples exhibit reverse zonation, whereas both normal- and reverse-zoned pyroxene phenocrysts coexist in the 1988–1989 samples (**Fig. 5**); and 4) the Ti-magnetite phenocrysts in the 1962 samples are nearly homogeneous from the core to the rim, whereas those in the 1988–1989 ones have Ti-rich and Mg-poor rims (**Figs. 5** and **6**).

The olivine microphenocrysts with Fe-rich cores (Fo < 70) in the 1988–1989 juvenile materials are usually surrounded by orthopyroxene and pigeonite [7]. The widths of the rims vary up to about 20 μm (**Fig. 3(a)**). These microphenocrysts are not in equilibrium with the high-Fo olivine (Fo > 75) from the basaltic magma; however, they are in equilibrium with both the orthopyroxene (Mg# 66–75) and clinopyroxene (Mg# 70–76) phenocrysts derived from the andesitic magma [25–27]. This suggests that the andesitic end-member magma of the 1988–1989 eruption contained Fe-rich olivine microphenocrysts, which was not recognized in the 1962 samples. Thus, it appears that the andesitic end-member magma of the 1988–1989 eruption is not strictly the same as that of the 1962 eruption. The presence of the Fe-rich olivine microphenocrysts and Ti-magnetite phenocrysts with lower Mg/Mn ratios in the 1988–1989 samples can be explained by the following processes. After the 1962 eruption, the remnant mixed magma existed in the magma chamber and underwent differentiated or cooling. During a period of more than 20 years, the Fe-rich olivine in equilibrium with the pyroxenes phenocrysts crystallized. At the same time, olivine microphenocrysts might have undergone element diffusion in the remnant magma. Moreover, a reaction between the olivine and the remnant mixed magma also occurred to form thick pyroxene reaction rims around the Fe-rich olivine (**Fig. 3(a)**). Further, compositional zonations of the pyroxenes phenocrysts (**Fig. 5**) could have been formed by the crystallization processes of the remnant mixed magma after the 1962 eruption. During crystallization, the magnetite phenocryst composition can change to achieve a lower Mg/Mn ratio because the diffusion rate of magnetite is quite high. In contrast, the core compositions of the pyroxene and plagioclase phenocrysts would not change significantly during the same duration (**Fig. 4**) because their diffusion rates are much lower than those of magnetite.

Conversely, the obvious compositional zonations in the Ti-magnetite phenocrysts might not have been caused by the crystallization processes of the remnant magma after the 1962 eruption. If the remnant magma stagnated in a deeper magma chamber after the 1962 eruption, the Ti-magnetite would simply grow as a homogeneous phenocryst. The possible processes that produce compositional zonations of Ti-magnetite phenocrysts will be discussed in the following section.

6.4. Origin of Overgrowth Rims of Ti-Magnetite Phenocrysts in the 1988–1989 Juvenile Materials

The timing of mafic injection has been discussed on the basis of the diffusion profile of the Ti-magnetite phenocryst rims [11, 28]. In such cases, the magnetite phenocrysts recorded the mafic injection occurrence within several days before the eruption. Although the mafic injection also occurred before the 1962 eruption, the Ti-magnetite phenocrysts in the rocks do not show compositional zonations at the rim zones (**Figs. 5** and **6**). This suggests that the diffusion profiles in the Ti-magnetite phenocrysts began to homogenize prior to the eruption. When the 10 μm mantle of high-Mg/Mn ($TiO_2 = 10.7$ wt.% with Mg/Mn $= 20$) was formed around the andesitic Ti-magnetite ($TiO_2 = 11.7$ wt.% with Mg/Mn $= 15$) by magma mixing, the TiO_2 in the Ti-magnetite began to become homogeneous for approximately two days under a compositionally independent diffusion model assuming a sphere, using $K_d = 1.49 \times 10^{-11}$ cm^2/s at $T = 1{,}000$°C and $X_{\mathrm{Ti}} = 0.1$ [29]. Moreover, complete homogeneity occurred in less than one week. Therefore, we conclude that the duration of several months between the injection of basaltic magma and eruption, estimated by the diffusion profiles of olivine phenocrysts, was long enough to homogenize the compositional profiles of the Ti-magnetite. Incidentally, the same process must have occurred prior to the 1988–1989 eruption. According to our analysis assuming the composition of andesitic Ti-magnetite as $TiO_2 = 12.3$ wt.% with Mg/Mn $= 13$, the TiO_2 in the Ti-magnetite become homogeneous for less than two weeks, using $K_d = 6.48 \times 10^{-12}$ cm^2/s at $T = 950$°C and $X_{\mathrm{Ti}} = 0.1$) [29]. This result also suggests the possibility of homogenization in the Ti-magnetite prior to the 1988–1989 eruption.

Conversely, the Ti-magnetite phenocrysts in the 1988–1989 samples exhibit mantle zoning, in which obvious profiles of the Mg/Mn ratio, X'_{usp}, and Al_2O_3 content

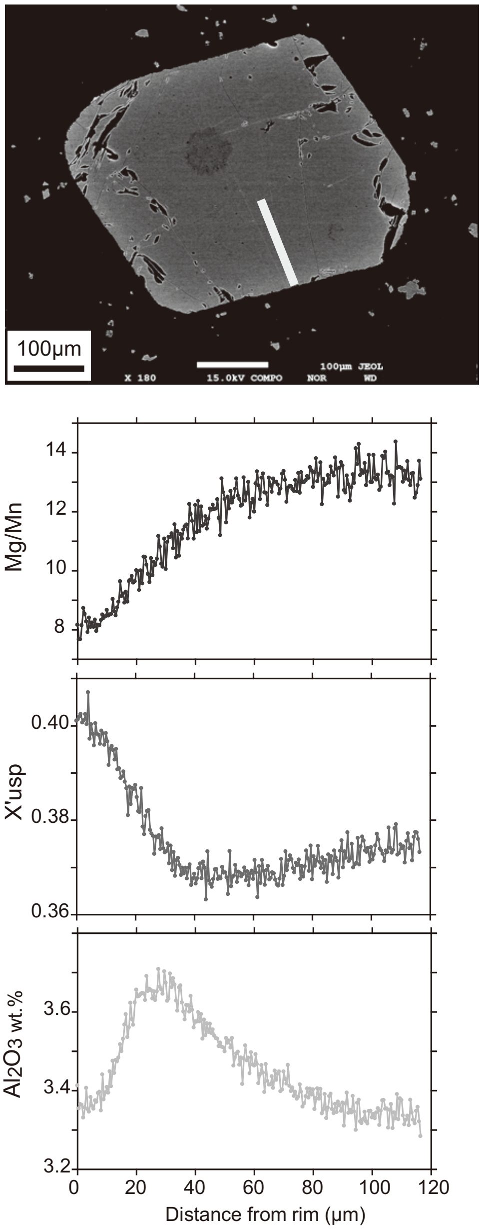

Fig. 9. Zoning profiles of Ti-magnetite phenocrysts in the 1988 sample. The light color bar indicates the profile.

are recognized (**Fig. 9**). The width of the zone is about several tens of microns (**Figs. 6** and **9**). The profile in **Fig. 9** is inconsistent with possible compositional zonation caused by simple magma mixing. The Al_2O_3 content increases toward the inner rim from the inside and decrease toward the outer rim. The zoning profile of the Al_2O_3 content (**Fig. 9**) cannot be formed by a simple diffusion process. Thus, the mantle zones around the Ti-magnetite phenocrysts in the 1988–1989 samples can be considered as an overgrowth zone rather than a diffusion zone. That is, these mantles were grown after the homogenization of the zoning caused by magma mixing.

Figure 10 shows the compositional relationship between the phenocrysts and microlites. The X'_{usp} values of the Ti-magnetite microlites of the 1962 samples are 0.34–0.46; the Mg/Mn ratios are between 8 and 12; and the Al_2O_3 content is 2.5–4.2; however, those of the 1988–1989 samples are 0.44–0.58, 5–6, and 2.0–2.6, respectively. Compared with the phenocryst rims of each sample, the microlites are rich in Ti and poor in Mg and Al compositions (**Fig. 10**). It is widely accepted that microlites crystallize during ascent from a magma chamber to the surface. Here, we refer to the crystallization stage of microlites as the microlite stage. In the case of the 1962 eruption, the chemical compositions of the rims of the phenocrysts and microlites changed continuously. This suggests that the mixed magma moved from the chamber, where the phenocrysts crystallized, to the microlite stage and indicates that the mixed magma ascended rapidly to the surface with no stagnation. On the contrary, the chemical compositions of the phenocryst mantle zones in the 1988–1989 samples are intermediate values between the cores of the phenocrysts and microlites. This suggests that the mantle zone matured between the magma chamber and the microlite stage. Moreover, the mantle zone, showing a width of about 50 μm in **Fig. 9**, is significantly wider than that of the microlites, about 10 μm in **Fig. 2(f)**. These results suggest that the mixed magma of the 1988–1989 eruption had a slower ascent than that of the 1962 eruption. During the ascent, magma can stagnate at the vent system. We speculate that the mantle zones of the Ti-magnetite phenocrysts formed during a slow ascent or stagnation, and the magma then finally ascended to the surface to erupt after the stagnation. We conclude that microlites crystallized during this final ascent.

During the 1988–1989 eruption, vent breccia blocks containing fresh mafic andesite dykes were formed. The dykes show the same petrological features as those of the 1988–1989 mafic andesite [7], which suggests that the magma slowly ascended and stagnated as dykes into the vent system. Ikeda et al. [7] also described that the matrix crystallinity of the 1988–1989 juvenile materials was significantly higher that of the 1962 ones. In addition, the diffusion profiles in the olivine microphenocrysts suggest that the duration between the basalt injection and the 1988–1989 eruption was longer than that of the 1962 eruption. These might support the speculation that the 1988–1989 eruptive magma had a slower ascent than that of the 1962 event. As previously mentioned, we speculated that the Fe-rich rims (Fo < 60) with thin reaction pyroxene rims around the high-Fo olivine (**Fig. 8(b)**) might also have formed during the same crystallization stage.

6.5. Eruption Processes of the 1962 and 1988–1989 Eruptions

The 1962 eruption was a major magmatic eruption of Tokachidake volcano [8]. The climactic episode was a sub-Plinian-type eruption that continued for less than 24 h. The eruption rate of the 1962 eruption was estimated to be on the order of 10^7 m^3/day based on the total volume of the eruption (7.1×10^7 m^3) [17]. On the contrary, the 1988–1989 eruption was a series of small Vulca-

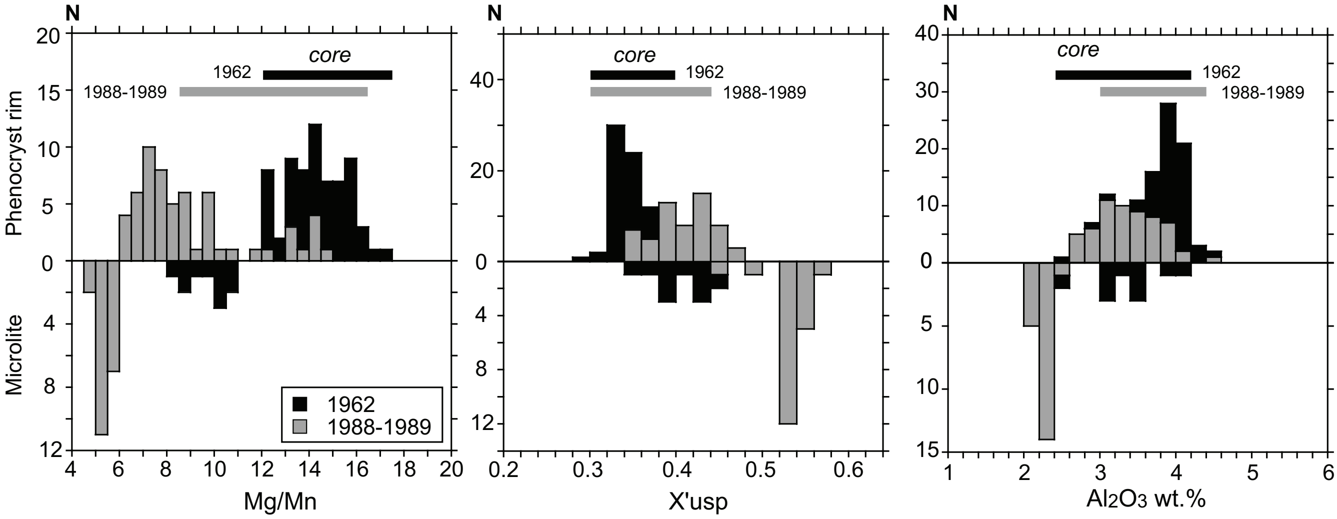

Fig. 10. Histograms of Mg/Mn ratio, X'_{usp}, and Al_2O_3 (wt.%) of the rims of Ti-magnetite phenocrysts and microlites from the 1962 and 1988–1989 samples. The ranges of the phenocryst cores are also shown as bars in the figure.

nian eruptions. The total volume of ejecta from its 23 Vulcanian explosions was estimated to be 6×10^5 m^3 [2]. Moreover, Katsui et al. [2] estimated the proportion of juvenile materials in the ejecta to be about 20%. Thus, the eruption magma volume during the 1988–1989 activity was likely 1.2×10^5 m^3 per 23 eruptions. Although the eruption rates of the 1988–1989 event could not be converted to the order of one day, the eruption rate must have differed significantly between the two eruptions. If the eruption rate is related to the ascent rate of the magma from the chamber to the surface, the ascent rates of the two eruptions should be quite different. The rate of the 1962 eruption, on the order of 10^7 m^3/day, was significantly larger than that of the 1988–1989 eruption, on the order of 10^3 m^3/eruption. This difference in ascent rate is consistent with our speculation based on petrological analysis of the juvenile materials.

The petrological analysis of the historic juvenile materials of Tokachidake volcano revealed the magma processes during the 20th century, as shown in **Fig. 11**. The magma system of the volcano is composed of two distinct magmas: andesitic and basaltic. In the case of the 1962 eruption, the basaltic magma was injected into the andesitic magma several months prior to the eruption (**Fig. 11(a)**). The existence of homogenized magnetite phenocrysts suggests that another injection did not occur within several days before the eruption. The preparation processes continued for at least several months after the injection of the basaltic magma. Then, the mixed magma rapidly ascended to erupt without stagnation (**Fig. 11(b)**). This speculation is supported by petrological features of the 1962 eruptive scoria, such as the glassy matrix, small sizes of microlite in the matrix, and olivine microphenocrysts without pyroxene reaction rims.

The remnant mixed magma stagnated in a magma chamber after the 1962 eruption (**Fig. 11(c)**). The crystallization processes and cooling of the remnant magma after the eruption produced petrographical features such as the co-existence of Fe-rich olivine surrounded by thick pyroxene rims and Mg-poor Ti-magnetite in the eruptive rocks of the 1988–1989 eruption (**Fig. 11(d)**). Then, the injection of the basaltic magma occurred about six months prior to the 1988–1989 eruption (**Fig. 11(e)**). After the homogenization of the Ti-magnetite, the mixed magma began to ascend slowly and might have stagnated within the vent system during the ascent (**Fig. 11(f)**). Formation of a mantle zone of Ti-magnetite phenocrysts and growth of thin pyroxene rims around high-Fo olivine can occur during a slow ascent or stagnation within a vent system. In such cases, the stagnant magma head would behave as a cap rock of the vent system; therefore, the explosive nature of the 1988–1989 eruptive activity might have been caused by formation and destruction of the cap rock (**Figs. 11(g)–(h)**).

7. Concluding Remarks

Although juvenile materials of both the 1962 and 1988–1989 eruptions are composed of similar mafic andesites, which is the product of magma mixing between basaltic and andesitic magmas, our petrological analysis revealed the existence of many petrographical and petrological differences between them. The magma processes that produced these features summarized below.

(1) Several months prior to the 1962 eruption, the basaltic magma was injected into the shallower andesitic magma chamber. Then, the mixed magma rapidly ascended from the chamber to the surface without stagnation and produced a sub-Plinian eruption.
(2) The remnant mixed magma was contained in the chamber after the 1962 eruption, where crystallization and cooling occurred.
(3) Another basaltic magma was injected into the rem-

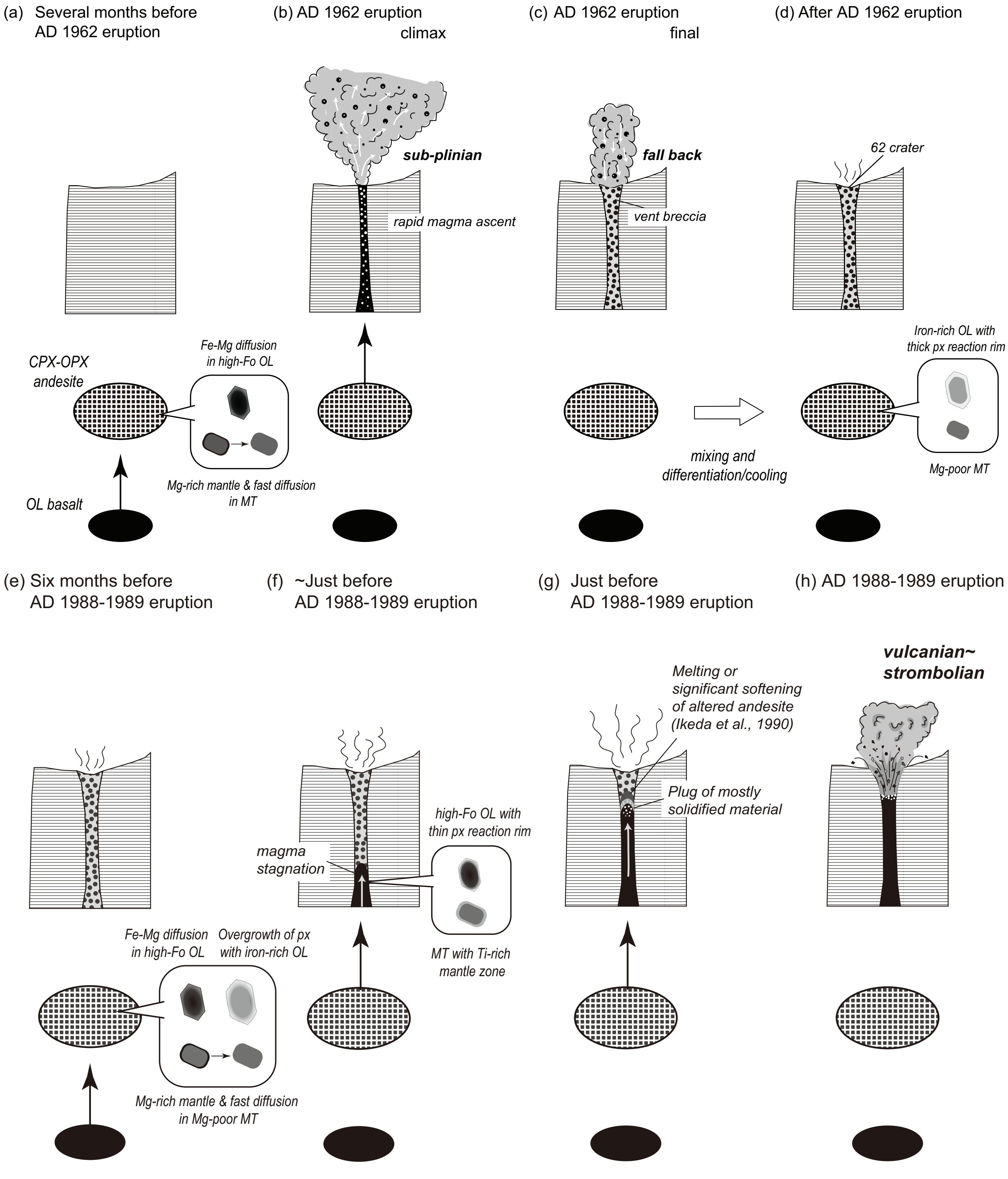

Fig. 11. Diagram of the eruption processes of the 1962 and 1988–1989 events. 1962 eruption: (a) several months prior to the eruption; (b) sub-Plinian eruption (climax stage); (c) fallback of ejecta (final stage); (d) after the eruption. 1988–1989 eruption: (e) six months before the eruption; (f) closer to the eruption; (g) just prior to the eruption; (h) Vulcanian eruption.

nant magma about six months prior to the 1988–1989 eruption. Then, the mixed magma slowly ascended and stagnated between the chamber and the surface. Finally, small Vulcanian explosions occurred intermittently for three months.

(4) Different modes of magma ascent caused the different eruption styles. In addition, evidence for the ascent rate differences is recorded in the eruptive materials.

In summary, we emphasize that petrological analysis of eruptive rocks can reveal their eruption processes. Systematic sampling and petrological analysis of dated eruptive materials for each eruption episode can be used to forecast the sequences of eruptive activity. To develop the forecasting of eruption and its sequences, case studies of previous eruptive activities must be accumulated and evaluated.

Acknowledgements

The authors thank H. Nomura and K. Nakamura for thin section preparation and two anonymous reviewers for offering constructive comments. This work was supported by a research grant from JSPS KAKENHI (Grant No. 15H03745 to MN) and by the Ministry of Education, Culture, Sports, Science and Technology (MEXT) of Japan under its "Earthquake and Volcano Hazards Observation and Research Program" and "Integrated Program for Next Generation Volcano Research and Human Resource Development."

References:

[1] T. Ishikawa, I. Yokoyama, Y. Katsui, and M. Kasahara, "Tokachi-dake, its volcanic geology, history of eruption, present state of activity and prevention of disasters," Committee for Prevention of the Natural Disasters of Hokkaido, Sapporo, 1971 (in Japanese with English abstract).

[2] Y. Katsui, S. Kawachi, Y. Kondo, Y. Ikeda, M. Nakagawa, Y. Gotoh, H. Yamagishi, T. Yamazaki, and M. Sumita, "The 1988-1989 explosive eruption of Tokachi-dake, central Hokkaido, its sequence and mode: Special Section: The 1988-1989 Eruption of Mt. Tokachi, Central Hokkaido," Bull. Volcanol. Soc. Japan, Vol.35, No.2, pp. 111-129, 1990.

[3] Y. Ishizuka, M. Nakagawa, and S. Fujiwara, "Geological map of Tokachidake volcano, 1:30,000," Geological Survey of Japan, p. 7, 2010.

[4] Japan Meteorological Agency, "10. Tokachidake," National catalogue of the active volcanoes in Japan (the 4th edition), pp. 1-39, 2013.

[5] R. Tanaka, T. Hashimoto, N. Matsushima, and T. Ishido, "Permeability-control on volcanic hydrothermal system: case study for Mt. Tokachidake, Japan, based on numerical simulation and field observation," Earth Planets Space, Vol.69, No.1, Article: 39, doi:10.1186/s40623-017-0623-5, 2017.

[6] R. Takahashi and M. Yahata, "Effects of subvolcanic hydrothermal systems on edifice collapses and phreatic eruptions at Tokachidake volcano, Japan," J. Volcanol. Geotherm. Res., Vol.352, pp. 117-129, 2018.

[7] Y. Ikeda, Y. Katsui, M. Nakagawa, S. Kawachi, T. Watanabe, N. Fujibayashi, T. Shibata, and H. Kagami, "Petrology of the 1988-89 essential ejecta and associated glassy rocks of Tokachi-dake volcano in central Hokkaido, Japan: Special Section: The 1988-1989 Eruption of Mt. Tokachi, Central Hokkaido," Bull. Volcanol. Soc. Japan, Vol.35, No.2, pp. 147-162, 1990.

[8] S. Fujiwara, M. Nakagawa, S. Hasegawa, and D. Komatsu, "Eruptive history of Tokachi-dake volcano during the last 3,300 years, Central Hokkaido, Japan," Bull. Volcanol. Soc. Japan, Vol.52, No.5, pp. 253-271, 2007 (in Japanese with English abstract).

[9] A. Tomiya and E. Takahashi, "Evolution of the magma chamber beneath Usu volcano since 1663: a natural laboratory for observing changing phenocryst compositions and textures," J. Petrol., Vol.46, No.12, pp. 2395-2426, 2005.

[10] A. Matsumoto and M. Nakagawa, "Formation and evolution of silicic magma plumbing system: Petrology of the volcanic rocks of Usu volcano, Hokkaido, Japan," J. Volcanol. Geotherm. Res., Vol.196, No.3-4, pp. 185-207, 2010.

[11] R. Takahashi and M. Nakagawa, "Evolution and eruption processes of a highly porphyritic silicic magma system: Petrology of the historical eruptive stage of Hokkaido-Komagatake volcano, Japan," J. Petrol., Vol.56, No.6, pp. 1089-1112, 2015.

[12] M. Amma-Miyasaka and M. Nakagawa, "Evolution of deeper basaltic and shallower andesitic magmas during AD 1469–1983 eruptions of Miyake-jima volcano, Izu-Mariana arc: Inferences from temporal variations of mineral compositions in crystal-clots," J. Petrol., Vol.44, No.12, pp. 2113-2138, 2003.

[13] Y. Suzuki, A. Yasuda, N. Hokanishi, T. Kaneko, S. Nakada, and T. Fujii, "Syneruptive deep magma transfer and shallow magma remobilization during the 2011 eruption of Shinmoe-dake, Japan – Constraints from melt inclusions and phase equilibria experiments," J. Volcanol. Geotherm. Res., Vol.257, pp. 184-204, 2013.

[14] A. Tomiya, I. Miyagi, G. Saito, and N. Geshi, "Short time scales of magma-mixing processes prior to the 2011 eruption of Shinmoedake volcano, Kirishima volcanic group, Japan," Bull. Volcanol., Vol.75, No.10, Article: 750, doi:10.1007/s00445-013-0750-1, 2013.

[15] S. Uesawa, "A study of the Taisho lahar generated by the 1926 eruption of Tokachidake volcano, central Hokkaido, Japan, and implications for the generation of cohesive lahars," J. Volcanol. Geotherm. Res., Vol.270, pp. 23-34, 2014.

[16] F. Tada and H. Tsuya, "The eruption of the Tokachidake volcano, Hokkaido, on May 24th, 1926," Bull. Earthq. Res. Inst. Univ. Tokyo, Vol.2, pp. 49-84, 1927 (in Japanese with English abstract).

[17] Y. Katsui, T. Takahashi, Y. Ôba, Y. Hirai, M. Iwanaga, T. Nishimura, T. Soya, and H. Itô, "1962 eruption of Tokachi-dake, Hokkaido," J. Japan Assoc. Mineral. Petrol. Econ. Geol., Vol.49, pp. 213-226, 1963 (in Japanese with English abstract).

[18] T. W. Sisson and T. L. Grove, "Experimental investigations of the role of H_2O in calc-alkaline differentiation and subduction zone magmatism," Contrib. Mineral. Petrol., Vol.113, No.2, pp. 143-166, 1993.

[19] D. Takagi, H. Sato, and M. Nakagawa, "Experimental study of a low-alkali tholeiite at 1–5 kbar: optimal condition for the crystallization of high-An plagioclase in hydrous arc tholeiite," Contrib. Mineral. Petrol., Vol.149, No.5, pp. 527-540, 2005.

[20] J. Crank, "The mathematics of diffusion," Second edition, Oxford University Press, 1975.

[21] S. Chakraborty, "Rates and mechanisms of Fe–Mg interdiffusion in olivine at 980°–1300°C," J. Geophys. Res. Solid Earth, Vol.102, No.B6, pp. 12317-12331, 1997.

[22] R. Dohmen, H. -W. Becker, and S. Chakraborty, "Fe-Mg diffusion in olivine I: experimental determination between 700 and 1,200°C as a function of composition, crystal orientation and oxygen fugacity," Phys. Chem. Minerals., Vol.34, pp. 389-407, 2007.

[23] L. A. Coogan, A. Hain, S. Stahl, and S. Chakraborty, "Experimental determination of the diffusion coefficient for calcium in olivine between 900°C and 1500°C," Geochim. Cosmochim. Acta, Vol.69, No.14, pp. 3683-3694, 2005.

[24] A. Jambon, P. Lussiez, R. Clocchiatti, J. Weisz, and J. Hernandez, "Olivine growth rates in a tholeiitic basalt: an experimental study of melt inclusions in plagioclase," Chem. Geol., Vol.96, No.3-4, pp. 277-287, 1992.

[25] P. L. Roeder and R. F. Emslie, "Olivine-liquid equilibrium," Contrib. Mineral. Petrol., Vol.29, No.4, pp. 275-289, 1970.

[26] D. R. Baker and D. H. Eggler, "Compositions of anhydrous and hydrous melts coexisting with plagioclase, augite, and olivine or low-Ca pyroxene from 1 atm to 8 kbar: application to the Aleutian volcanic center of Atka," Am. Min., Vol.72, No.1-2, pp. 12-28, 1987.

[27] P. Beattie, "Olivine-melt and orthopyroxene-melt equilibria," Contrib. Mineral. Petrol., Vol.115, No.1, pp. 103-111, 1993.

[28] M. Nakamura, "Continuous mixing of crystal mush and replenished magma in the ongoing Unzen eruption," Geology, Vol.23, No.9 pp. 807-810, 1995.

[29] R. Freer and Z. Hauptman, "An experimental study of magnetite-titanomagnetite interdiffusion," Phys. Earth Planet. In., Vol.16, No.3, pp. 223-231, 1978.

Name:
Mitsuhiro Nakagawa

Affiliation:
Professor, Graduate School of Science, Hokkaido University

Address:
N10W8 Kita-ku, Sapporo, Hokkaido 060-0810, Japan

Brief Career:
1989-2004 Assistant Professor, Graduate School of Science, Hokkaido University
1995-1997 Visiting Scientist, Institute of Geological and Nuclear Sciences Limited
2004- Professor, Graduate School of Science, Hokkaido University

Selected Publications:
- "Evolution of the 120 ka caldera-forming eruption of Kutcharo volcano, eastern Hokkaido, Japan: Geologic and petrologic evidence for multiple vent systems and rapid generation of pyroclastic flow," J. Volcanol. Geotherm. Res., Vol.321, pp. 58-72, 2016.
- "Evolution and eruption processes of a highly porphyritic silicic magma system: Petrology of the historical eruptive stage of Hokkaido-Komagatake volcano, Japan," J. Petrol., Vol.56, No.6, pp. 1089-1112, 2015.
- "Formation of a zoned magma chamber and its temporal evolution during the historic eruptive activity of Tarumai Volcano, Japan: Petrological implications for a long-term forecast of eruptive activity of an active volcano," J. Volcanol. Geotherm. Res., Vol.205, No.1-2, pp. 1-16, 2010.

Academic Societies & Scientific Organizations:
- Volcanological Society of Japan (VSJ)
- Japan Geosciences Union (JpGU)
- International Association of Volcanology and Chemistry of the Earth's Interior (IAVCEI)
- American Geophysical Union (AGU)

Name:
Akiko Matsumoto

Affiliation:
Technical Staff, Graduate School of Science, Hokkaido University

Address:
N10W8 Kita-ku, Sapporo, Hokkaido 060-0810, Japan

Brief Career:
2006-2007 Postdoctoral Fellow, Graduate School of Science, Hokkaido University
2007- Technical Staff, Graduate School of Science, Hokkaido University

Selected Publications:
- "Reconstruction of the eruptive history of Usu volcano, Hokkaido, Japan, inferred from petrological correlation between tephras and dome lavas," Island Arc, Vol.28, No.3, e12301, 2019.
- "Petrology of the 120 ka caldera-forming eruption of Kutcharo volcano, eastern Hokkaido, Japan: Coexistence of multiple silicic magmas and their relationship with mafic magmas," J. Petrol., Vol.59, No.4, pp. 771-793, 2018.

Academic Societies & Scientific Organizations:
- Volcanological Society of Japan (VSJ)
- Geological Society of Japan (JGS)

Name:
Kyohei Kobayashi

Affiliation:
Koken Engineering Co., Ltd.

Address:
1-1 N18E17, Higashi-ku, Sapporo, Hokkaido 065-8510

Brief Career:
2015-2017 Master Course, Graduate School of Science, Hokkaido University
2017- Koken Engineering Co., Ltd.

Name:
Keiji Wada

Affiliation:
Professor, Hokkaido University of Education

Address:
9 Hokumon-cho, Asahikawa, Hokkaido 070-8621, Japan

Brief Career:
1983- Hokkaido University of Education

Selected Publications:
- "Fractal structure of heterogeneous ejecta from the Me-akan volcano, eastern Hokkaido, Japan: implications for mixing mechanism in a volcanic conduit," J. of Volcanology and Geothermal Research, Vol.66, No.1-4, pp. 69-79, 1995.

Academic Societies & Scientific Organizations:
- Volcanological Society of Japan (VSJ)
- Geological Society of Japan (JGS)
- International Association of Volcanology and Chemistry of the Earth's Interior (IAVCEI)